

Manifestation of α -clustering in ^{10}Be via α -knockout reaction

Mengjiao Lyu,^{1,*} Kazuki Yoshida,^{1,†} Yoshiko Kanada-En'yo,^{2,‡} and Kazuyuki Ogata^{1,§}

¹Research Center for Nuclear Physics (RCNP), Osaka University, Ibaraki 567-0047, Japan

²Department of Physics, Kyoto University, Kyoto 606-8502, Japan

(Dated: October 3, 2018)

Background Proton-induced α -knockout reactions may allow direct experimental observation of α -clustering in nuclei. This is obtained by relating the theoretical descriptions of clustering states with experimental reaction observables. It is desired to introduce microscopic structure models into the theoretical frameworks for α -knockout reactions.

Purpose Our goal is to probe the α -clustering in ^{10}Be nucleus by proton-induced α -knockout reaction observables.

Method We adopt an extended version of the Tohsaki-Horiuchi-Schuck-Röpke (THSR) wave function of ^{10}Be and integrate it with the distorted wave impulse approximation (DWIA) framework for the calculation of $(p, p\alpha)$ knockout reactions.

Results We make the first calculation for the $^{10}\text{Be}(p, p\alpha)^6\text{He}$ reaction at 250 MeV implementing a microscopic α -cluster wave function and predict the triple differential cross sections (TDX). Furthermore, by constructing artificial states of the target nucleus ^{10}Be with compact or dilute spatial distributions, the TDX is found to be highly sensitive to the extent of clustering in the target nuclei.

Conclusions These results provide reliable manifestation of the α -clustering in ^{10}Be .

PACS numbers: 24.10.Eq, 25.40.-h

I. INTRODUCTION

Clustering is one of the fundamental degrees of freedom in nuclei [1] that originates from the delicate balances between Pauli blocking effects and nucleon-nucleon interactions in nuclear many-body dynamics [2]. Hence, a microscopic description, which takes into account both the nucleon degrees of freedom in interactions and the total antisymmetrization, is essential for the study of nuclear clustering states. In recent years, the microscopic theories have been well established for clustering states ranging from the molecular-like states in $^9,^{10}\text{Be}$ [3–18] to the gas-like Hoyle state (0_2^+) in ^{12}C [19–23]. In these studies, physical observables such as energies and radii are calculated for the clustering states and the corresponding experimental values are well reproduced. This indicates the validity of the α -clustering picture for these states. However, physical observables that are directly related to the cluster degree of freedom will be necessary for an evident manifestation of clustering in nuclei.

It is expected that nuclear reactions with adding or removing α -cluster(s) provide direct probe of α -clustering in nuclei [24–26]. In recent work, microscopic cluster model based on the generator coordinate method has been introduced into the theoretical framework of α -transfer reactions and it significantly improves the prediction of transfer cross sections [24]. The α -knockout reaction, which is an alternative approach, has been adopted for the investigation of α -clustering in stable nuclei for decades [25–33]. In these studies, the distorted wave impulse approximation (DWIA) has been adopted by employing phenomenological α -cluster wave functions. Using a hydrogen target, the $(p, p\alpha)$ reaction can be applied to studies on α -clustering in unstable nuclei, which is a hot subject in nuclear physics [14, 34–36]. In a recent theoretical study [25], the so-called factorization approximation which has frequently been made in DWIA framework is validated. Furthermore, corresponding DWIA calculations with phenomenological α -cluster wave functions have shown the peripheral property of the α -knockout reaction, which lays the foundations for directly probing α -clustering in the surface region of nuclei [25, 26]. Hence, it is appealing and promising to integrate the microscopic clustering models into this DWIA framework and make microscopic predictions for the α -knockout reaction observables.

In the present work, we study the α -knockout reaction $^{10}\text{Be}(p, p\alpha)^6\text{He}$ at 250 MeV. The microscopic cluster models for the ^{10}Be nucleus are already well established and its ground state is predicted to be molecular-like. Along this line, measurement of proton-induced α -knockout reactions for Be isotopes in inverse kinematics is planned at RIBF [37]. Thus, the $^{10}\text{Be}(p, p\alpha)^6\text{He}$ knockout reaction at 250 MeV will be an ideal choice for the manifestation of α -clustering. In our calculations, we adopt the extended version of the Tohsaki-Horiuchi-Schuck-Röpke (THSR) wave function [19] for the description of target nucleus ^{10}Be and the residual nucleus ^6He [18, 38], and then integrate it into the DWIA framework to predict the $^{10}\text{Be}(p, p\alpha)^6\text{He}$ reaction observables. Furthermore, benefiting from the flexible model space in the THSR wave function, we can smoothly evolve the

*mengjiao@rcnp.osaka-u.ac.jp

†yoshidak@rcnp.osaka-u.ac.jp

‡yeny@ruby.scphys.kyoto-u.ac.jp

§kazuyuki@rcnp.osaka-u.ac.jp

physical ground state of ^{10}Be into artificial states of cluster gas-like limit with large spatial spread or compact SU(3)-shell-model limit. This is obtained by controlling one parameter for the α -cluster distribution size (the α -cluster motion) in the THSR wave function. By investigating the dependence of reaction observables on the α -cluster motion, it is presented that the α -knockout reaction is a sensitive probe to distinguish the shell-model limit, the molecular-like, or the gas-like cluster state, and can thus provide direct manifestation of nuclear structures in ^{10}Be .

This article is organized as follows. In Section II, we introduce the theoretical framework for the α -knockout reaction: the DWIA for calculating transition amplitudes and triple differential cross sections (TDX), and the THSR wave function for the microscopic description of target and residual nuclei. In Section III, we show the numerical inputs and discuss the results of both structures and reaction observables. Last Section IV contains the conclusion.

II. FORMALISM

We integrate the DWIA framework and the THSR wave function to formulate a microscopic description of the $^{10}\text{Be}(p,p\alpha)^6\text{He}$ knockout reaction.

A. DWIA framework for the $^{10}\text{Be}(p,p\alpha)^6\text{He}$ reaction

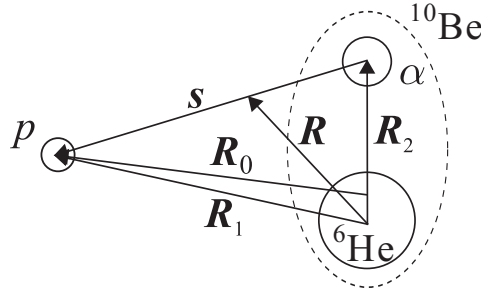


FIG. 1: Coordinates of the $^{10}\text{Be}(p,p\alpha)^6\text{He}$ reaction.

We adopt the normal kinematics for the $^{10}\text{Be}(p,p\alpha)^6\text{He}$ reaction in the DWIA framework. The transition amplitude is given by

$$T_{\mathbf{K}_0\mathbf{K}_1\mathbf{K}_2} = \left\langle \chi_{1,\mathbf{K}_1}^{(-)}(\mathbf{R}_1) \chi_{2,\mathbf{K}_2}^{(-)}(\mathbf{R}_2) | t_{p\alpha}(s) | \chi_{0,\mathbf{K}_0}^{(+)}(\mathbf{R}_0) \varphi_\alpha(\mathbf{R}_2) \right\rangle. \quad (1)$$

Here, the incident proton p , the outgoing p , and the outgoing α are labeled by 0, 1, and 2, respectively, and the distorted waves χ are specified with these numbers in subscripts. The coordinates are given in Fig. 1. The momentum and its solid angle of each particle are denoted by \mathbf{K}_i and Ω_i ($i = 0, 1, 2$), respectively. Quantities with superscript L are evaluated in the laboratory frame, and others are evaluated in the center-of-mass frame. The superscripts (+) and (-) on χ indicate that the outgoing- and incoming-wave boundary conditions are adopted, respectively. The optical potential for each system is given by folding density distributions of ^{10}Be and ^6He which are predicted by the THSR wave function (see Sec. II B) with an effective nucleon-nucleon (NN) interaction. The three distorted wave functions are then obtained by solving the corresponding Schrödinger equations. φ_α is the α -cluster wave function inside ^{10}Be nucleus with total angular momentum $j = 0$ and parity $\pi = +$. This α -cluster wave function is extracted from the THSR wave function of ^{10}Be by approximating the reduced width amplitude (RWA). Hence, all the wave functions used in the calculation of transition amplitude are microscopically obtained. The transition interaction $t_{p\alpha}$ between p and α is obtained by a folding model calculation as in Ref. [25].

As illustrated in Ref. [25], with the asymptotic momentum approximation, the reduced transition amplitude $\bar{T}_{\mathbf{K}_0\mathbf{K}_1\mathbf{K}_2}$ can be expressed as

$$\bar{T}_{\mathbf{K}_0\mathbf{K}_1\mathbf{K}_2} = \int d\mathbf{R} F_{\mathbf{K}_0\mathbf{K}_1\mathbf{K}_2}(\mathbf{R}) \varphi_\alpha(\mathbf{R}), \quad (2)$$

where $F_{\mathbf{K}_0\mathbf{K}_1\mathbf{K}_2}(\mathbf{R})$ is defined by

$$F_{\mathbf{K}_0\mathbf{K}_1\mathbf{K}_2}(\mathbf{R}) \equiv \chi_{1,\mathbf{K}_1}^{*(-)}(\mathbf{R}) \chi_{2,\mathbf{K}_2}^{*(-)}(\mathbf{R}) \times \chi_{0,\mathbf{K}_0}^{(+)}(\mathbf{R}) e^{-i\mathbf{K}_0(\mathbf{R})\cdot\mathbf{R}(4/10)}. \quad (3)$$

With $\bar{T}_{\mathbf{K}_0\mathbf{K}_1\mathbf{K}_2}$ in Eq. (2), the triple differential cross section (TDX) of the $^{10}\text{Be}(p, p\alpha)^6\text{He}$ reaction is given by

$$\frac{d^3\sigma}{dE_1^L d\Omega_1^L d\Omega_2^L} = F_{\text{kin}} C_0 \frac{d\sigma_{p\alpha}}{d\Omega_{p\alpha}}(\theta_{p\alpha}, E_{p\alpha}) |\bar{T}_{\mathbf{K}_0\mathbf{K}_1\mathbf{K}_2}|^2. \quad (4)$$

$\theta_{p\alpha}$ is the scattering angle of the p - α binary collision and $E_{p\alpha}$ is its scattering energy defined by

$$E_{p\alpha} = \frac{\hbar^2 \kappa'^2}{2\mu_{p\alpha}}, \quad (5)$$

where $\mu_{p\alpha}$ is the reduced mass of the p - α system and κ' is the asymptotic relative momentum between emitted p and α -cluster in the final channel. F_{kin} in Eq. (4) is the kinematical factor defined as

$$F_{\text{kin}} = J_L \frac{K_1 K_2 E_1 E_2}{\hbar^4 c^4} \left[1 + \frac{E_2}{E_B} + \frac{E_2(\mathbf{K}_1 \cdot \mathbf{K}_2)}{E_B K_2^2} \right]^{-1}, \quad (6)$$

where J_L is the Jacobian from the center-of-mass frame to the laboratory frame, E_i and E_B denote the total energy of particle i and that of ^6He , respectively. C_0 in Eq. (4) is a coefficient given by

$$C_0 = \frac{E_0}{(\hbar c)^2 K_0} \frac{\hbar^4}{(2\pi)^3 \mu_{p\alpha}^2}. \quad (7)$$

B. THSR wave function for the target and residual nuclei

We use the latest version of the THSR wave function in Ref. [38] with a di-neutron pairing term for the descriptions of a nucleus A, which is ^6He or ^{10}Be , as

$$|\Phi(\text{A})\rangle = \hat{P}_{MK}^J (C_\alpha^\dagger)^{(1,2)} \left[(1 - \gamma) c_{n,\uparrow}^\dagger c_{n,\downarrow}^\dagger + \gamma c_{2n}^\dagger \right] |\text{vac}\rangle. \quad (8)$$

Here, $|\text{vac}\rangle$ is the vacuum state from which the α clusters and valence neutrons are created. Indices 1 and 2 in $(C_\alpha^\dagger)^{(1,2)}$ correspond to the residual nucleus ^6He and target nucleus ^{10}Be , respectively.

C_α^\dagger is the creation operators of α -clusters with the form of

$$C_\alpha^\dagger = \int d\mathbf{R} \exp\left(-\frac{R_x^2 + R_y^2}{\beta_{\alpha,xy}^2} - \frac{R_z^2}{\beta_{\alpha,z}^2}\right) \int d\mathbf{r}_1 \cdots d\mathbf{r}_4 \times \psi(\mathbf{r}_1 - \mathbf{R}) a_{\sigma_1, \tau_1}^\dagger(\mathbf{r}_1) \cdots \psi(\mathbf{r}_4 - \mathbf{R}) a_{\sigma_4, \tau_4}^\dagger(\mathbf{r}_4), \quad (9)$$

where \mathbf{R} is the generator coordinate of the α -cluster and $\psi(\mathbf{r}_i - \mathbf{R}) a_{\sigma_i, \tau_i}^\dagger(\mathbf{r}_i)$ is the single nucleon state of the i th nucleon in the operator form with spin-isospin (σ, τ) , and with the spatial part of a Gaussian form as $\psi(\mathbf{r}) = (\pi b^2)^{-3/4} \exp[-r^2/(2b^2)]$. The parameter b is chosen to be 1.35 fm which reproduces the size of an isolated α particle. $\beta_{\alpha,xy}$ and $\beta_{\alpha,z}$ are deformed parameters for the nonlocalized motion of α -clusters. For each nucleus, the parameters $\beta_{\alpha,xy}$ and $\beta_{\alpha,z}$ are determined by variational calculation.

For the valence neutrons, two types of creation operators are used with or without the di-neutron pairing. The creation operator $c_{n,\sigma}^\dagger$ for the independent configuration of valence neutrons is given by

$$c_{n,\sigma}^\dagger = \int d\mathbf{R}_n \exp\left(-\frac{R_{n,x}^2 + R_{n,y}^2}{\beta_{n,xy}^2} - \frac{R_{n,z}^2}{\beta_{n,z}^2}\right) \int d\mathbf{r}_i \times (\pi b^2)^{-3/4} e^{(-1)^m \phi(\mathbf{R}_n)} e^{-(\mathbf{r}_i - \mathbf{R}_n)^2/(2b^2)} a_\sigma^\dagger(\mathbf{r}_i). \quad (10)$$

Here, the generator coordinate \mathbf{R}_n , parameters $\beta_{i,xy}$ and $\beta_{i,z}$ for valence neutrons are defined similarly to those in Eq. (9). $a_\sigma^\dagger(\mathbf{r}_i)$ is the single neutron creation operator at \mathbf{r}_i with spin σ . The phase factor $\exp[(-1)^m \phi(\mathbf{R}_n)]$ is used to describe the intrinsic negative parity of the π -orbit state for the valence nucleons as discussed in Refs. [17, 18], where m is the third component of the orbital angular momentum of the valence nucleon and $\phi(\mathbf{R}_i)$ is the azimuthal angle of \mathbf{R}_i . For the pairing configuration of valence nucleons, the creation operator c_{2n}^\dagger has the form

$$\begin{aligned} c_{2n}^\dagger &= \int d\mathbf{R}_{2n} \exp\left(-\frac{R_{2n,x}^2 + R_{2n,y}^2}{\beta_{2n,xy}^2} - \frac{R_{2n,z}^2}{\beta_{2n,z}^2}\right) \int d\mathbf{r}_i d\mathbf{r}_j \\ &\times (\pi b^2)^{-3/4} e^{-(\mathbf{r}_i - \mathbf{R}_{2n})^2 / (2b^2)} a_\uparrow^\dagger(\mathbf{r}_i) \\ &\times (\pi b^2)^{-3/4} e^{-(\mathbf{r}_j - \mathbf{R}_{2n})^2 / (2b^2)} a_\downarrow^\dagger(\mathbf{r}_j), \end{aligned} \quad (11)$$

where the generator coordinate \mathbf{R}_{2n} , parameters $\beta_{2n,xy}$ and $\beta_{2n,z}$ for di-neutron pair are similarly defined to those in Eq. (9). The mixture between the pairing and un-pairing configurations for the two valence neutrons are determined by the parameter γ . Parameters $\beta_{n,xy}$, $\beta_{n,z}$, $\beta_{2n,xy}$, $\beta_{2n,z}$ and γ are described by the variational calculation. Finally, we use the angular momentum projection operator \hat{P}_{MK}^J to restore the rotational symmetry of wave function [39].

In Eq. (8), the THSR wave functions are expressed ultimately by the creation operators of single nucleons, which consider explicitly the single-nucleon degrees of freedom including the antisymmetrization of all the nucleons. Because of the antisymmetrization, the formation of α -clusters in the inner region of the nucleus is suppressed in the present microscopic description, even though we explicitly write the wave function of ^{10}Be with the form of α -cluster creation operators. Hence, the so-called spectroscopic factor S_α for the THSR wave function is smaller than unity in general. The antisymmetrization effect is weak in the nuclear surface region where the α -knockout reaction takes place. It should be noted, however, that the Pauli blocking effects in the inner region will affect the α -cluster dynamics for the entire space. Thus, only with the microscopic description of cluster states, the amplitude of α -cluster wave function in the surface region can be correctly produced.

We extract the α -cluster wave function in the surface region from the THSR wave function of ^{10}Be . This is obtained by approximating the α -cluster RWA using the method proposed in Ref. [40] which is found to be successful in evaluating the RWA in α -decay width calculations. In this method, the RWA $y(a)$ at the channel radius a is approximated by $y^{\text{app}}(a)$ which is given by the overlap between the microscopic wave function of target nucleus and a Brink-Bloch wave function as

$$\begin{aligned} |ay(a)| &\approx ay^{\text{app}}(a) \\ &\equiv \frac{1}{\sqrt{2}} \left(\frac{6 \times 4}{10\pi b^2}\right)^{1/4} \left| \left\langle \Phi(^{10}\text{Be}) | \Phi_{\text{BB}}^{(0+)}(^6\text{He}, \alpha, S = a) \right\rangle \right|. \end{aligned} \quad (12)$$

Here $\Phi(^{10}\text{Be})$ is the THSR wave function of ^{10}Be , and $\Phi_{\text{BB}}(^6\text{He}, \alpha, S)$ is the Brink-Bloch-type wave function [41] for the two-body system composed by the residual nucleus ^6He and the α -cluster with the distance parameter S between these two components, as

$$\left| \Phi_{\text{BB}}^{(0+)}(^6\text{He}, \alpha, S) \right\rangle = \hat{P}_{00}^0 \left| \phi\left(\alpha, \frac{6}{10} S \vec{e}_z\right) \Phi(^6\text{He}(0^+), -\frac{4}{10} S \vec{e}_z) \right\rangle. \quad (13)$$

This wave function is projected onto angular momentum $J = 0$ and parity $\pi = +$ eigenstates corresponding to the desired quantum numbers for the ground state of ^{10}Be . The THSR wave function $\Phi(^6\text{He})$ projected into 0^+ state is adopted in this Brink-Bloch-type wave function Φ_{BB} for the description of the ^6He component. $y^{\text{app}}(a)$ is an approximated RWA of the α -cluster in ^{10}Be , which is regarded as the α -cluster wave function in the surface region.

It is already illustrated in Ref. [40] that the approximated RWA $y^{\text{app}}(a)$ in Eq. (12) is valid only for the outer region of nuclei. However, benefiting from the high selectivity of the nuclear surface region in $(p, p\alpha)$ knockout reaction [25, 26], this approximation will not affect the calculation of the α -knockout reaction as shown below.

III. RESULTS AND DISCUSSION

A. Numerical inputs

We study the $^{10}\text{Be}(p, p\alpha)^6\text{He}$ reaction at 250 MeV by taking the following kinematical conditions; the Madison convention is adopted. The kinetic energy of particle 1 is fixed at 180 MeV and its emission angle is set to $(\theta_1, \phi_1) = (60.9^\circ, 0^\circ)$. As for particle 2, ϕ_2 is fixed at 180° and θ_2 is varied around 51° to which the kinetic energy of particle 2 changes accordingly around 62.5 MeV. For the p - α system, the scattering angle $\theta_{p\alpha}$ varies around 76° and the scattering energy $E_{p\alpha}$ varies around 242 MeV. For all the scattering particles, the relativistic kinematics is adopted.

In the microscopic calculation of the ground state wave functions of ^{10}Be and ^6He , we follow Ref. [11] for the choice of the nucleon-nucleon interactions; we adopt the Volkov No. 2 interaction [42] for the central term and the G3RS interaction [43] for the spin-orbit term. All the variational parameters within the THSR wave function are optimized by variational calculation for the ground state energies of ^{10}Be and ^6He .

We employ the Melbourne g matrix [44] as an effective NN interaction in the folding model calculation for the optical potentials. For the α - ^6He potential, we adopt the target-density approximation proposed in Ref. [45].

B. Nuclear structure results

With the optimized THSR wave function, we obtain the energy of -61.4 MeV for the ground state of ^{10}Be . The extended version of the THSR wave function described in Sec. II B improves the ground state energy of ^{10}Be by about 1.0 MeV compared with the original one used in the previous study [18]. The corresponding root-mean-square charge radius is 2.31 fm which agrees very well with the recent experimental value of 2.36 fm [46]. Considering that the protons are only included in the α -clusters inside the ^{10}Be nucleus, this good agreement shows that the α -cluster motion is correctly described by the THSR wave function. The parameters $\beta_{\alpha,xy}$ and $\beta_{\alpha,z}$ defined in Eq. (9) describe the α -cluster motion in ^{10}Be nucleus. They are optimized in the variational calculation with values $\beta_{\alpha,xy} = 0.1$ fm and $\beta_{\alpha,z} = 2.6$ fm. Other parameters are also variationally determined.

Fig. 2(b) shows the intrinsic charge distribution for the cluster structures of ^{10}Be , from which a molecular like structure with two α -clusters located at a moderate distance is clearly observed. For comparison, we also show the charge distribution of two artificial states of ^{10}Be which are constructed by changing the parameter $\beta_{\alpha,z}$ by hand from the optimized value into two extreme values, $\beta_{\alpha,z} = 1.0$ fm and $\beta_{\alpha,z} = 6.0$ fm, as shown in Figs. 2(a) and (c), respectively. In Fig. 2(a), since the α -cluster motion is confined by the small parameter $\beta_{\alpha,z} = 1.0$ fm, a very compact distribution is observed with spatial overlap between the two α -clusters. In this case, the effect from antisymmetrization is very strong and the 2α wave function is almost equal to the SU(3)-shell-model limit. Hence, we call this the shell-model like state. On the other hand, in Fig. 2(c), a very dilute structure is observed for the two α -clusters with large distance between them. Hence, we call this the gas-like cluster state. In Figs. 2(a)–(c), a continuous evolution of the nuclear structure from the shell-model limit to the molecular-like state and then into the gas-like cluster state is observed. By predicting the physical observables of the $^{10}\text{Be}(p,p\alpha)^6\text{He}$ knockout reaction, we provide experimental probes for the effective distinguishment of these three cases of ^{10}Be nucleus.

In Fig. 3, we show the approximated RWA ($y^{\text{app}}(a)$) extracted from the THSR wave function for the three cases. Clear deviations are observed in the curves for different $\beta_{\alpha,z}$ parameters. This shows a dramatic difference on the α -cluster motions between the shell-model like, molecular-like, and gas-like cluster states, as discussed above. The present approximation of the RWA is valid in the surface and outer regions free from the antisymmetrization, but not in the inner region, in which the RWA should be strongly suppressed by the antisymmetrization. In the ^{10}Be wave function, the suppression is mainly contributed by the antisymmetrization of nucleons between two α -clusters. In Ref. [40], it is shown that the antisymmetrization between the two α -clusters in ^8Be is weak enough for $a \geq 3$ – 4 fm, which can be regarded as the physical region for two α -clusters. As shown later, the α -knockout reaction can selectively probe the clustering in the outer region, in which the RWA is safely approximated. The $y^{\text{app}}(a)$ in the ^{10}Be wave function in this physical region ($a \geq 3$ – 4 fm) shows a clear difference of clustering behavior between the three states. Namely, the amplitude is remarkably enhanced and reduced in the gas-like cluster and shell-model like states, respectively.

C. Nuclear reaction results

We show in Fig. 4 the calculated TDX for the physical ground state of ^{10}Be (blue solid line) compared with the results for two artificial states (green dashed and red dash-dotted line). We see giant ratio of about 10 for the TDXs around the peak between the shell-model like state ($\beta_{\alpha,z} = 1.0$ fm) and the molecular-like state ($\beta_{\alpha,z} = 2.6$ fm), and between the molecular-like state and the gas-like cluster state ($\beta_{\alpha,z} = 6.0$ fm). This shows that the TDX observables are very sensitive to the evolution of cluster structures of the ^{10}Be nucleus. By comparing the theoretical results of TDX with future experimental values, one may easily pin down the clustering structure in the physical ground state of ^{10}Be , which should be the molecular-like case according to the suggestion by microscopic theories. We see very large peak of the TDX for the gas-like cluster case and very small peak for the shell-model like case. This is reasonable because the α -clusters are remarkably enhanced in the gas-like cluster case and suppressed by Pauli blocking effects in the shell-model like case.

Next we discuss the peripheral property of the $^{10}\text{Be}(p,p\alpha)^6\text{He}$ knockout reaction by showing in Fig. 5 the transition matrix density (TMD) corresponding to $P_R = 0$. The TMD is the transition strength as a function of R as defined in Ref. [33]. It is clearly observed that the major contributions come from the middle and tail regions of the physical or artificial nuclei, which clearly shows the peripheral property of the knockout reaction as discussed in Refs. [25, 26]. This is essential for probing only the “physical” α -clustering in the surface and outer regions, in which α -clusters are free from the antisymmetrization effect, separating from those in the inner region where the α -clusters are not well defined because of the strong antisymmetrization

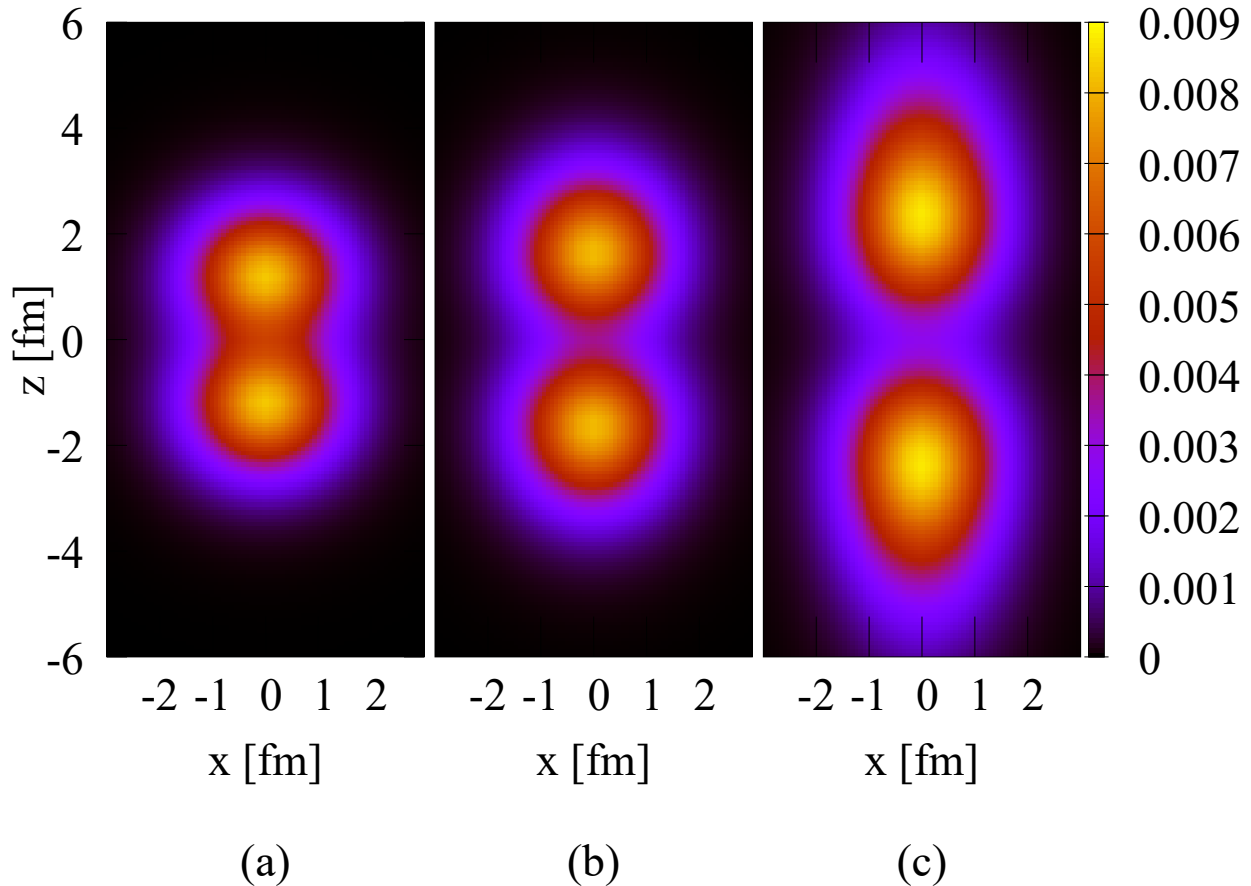


FIG. 2: Charge distribution of ^{10}Be nucleus for the (a) artificial shell-model like state with parameter $\beta_{\alpha,z} = 1.0$ fm, (b) the physical ground state with variational optimized parameter $\beta_{\alpha,z} = 2.6$ fm, and (c) artificial gas-like cluster state with parameter $\beta_{\alpha,z} = 6.0$ fm. (Color online)

effect. As mentioned above, the approximated α -cluster RWA is reliable only in the surface and outer regions. Nevertheless, we may conclude from Fig. 5 that the TMD has significant distribution only in the outer region where the approximated RWA adopted is reliable. Therefore, it will be expected that the features of the TDX for three states in Fig. 4 persist.

In previous studies of clustering physics, it is difficult to obtain direct experimental evidence of α -clustering. With our microscopic α -knockout reaction framework, we are able to detect directly the α -clustering in the surface region of nuclei. Furthermore, distinguishment between the compact molecular-like and gas-like cluster states is also possible in this new framework.

IV. SUMMARY

We have proposed the first microscopic framework for the study of $(p, p\alpha)$ knockout reaction by integrating a microscopic clustering model into the DWIA framework. With this new framework, we investigated the α -knockout reaction $^{10}\text{Be}(p, p\alpha)^6\text{He}$ at 250 MeV. The target nucleus ^{10}Be and the residual nucleus ^6He in this reaction are described microscopically by the THSR wave function. An approximated α -cluster RWA $y^{\text{app}}(a)$ is extracted from the THSR wave function of target nucleus ^{10}Be following Ref. [40], and implemented in the reaction calculation. By predicting the TDX for the $^{10}\text{Be}(p, p\alpha)^6\text{He}$ reaction, we have provided possibility for the direct manifestation of the α -clustering in ^{10}Be . We also compared the structures and reaction observables for the physical and two artificial states of the target nucleus ^{10}Be , namely the molecular-like, shell-model limit, and gas-like cluster states. The α -cluster amplitudes for these three states are very different from each other. In consequence of this, we observed giant ratio between their reaction observable TDXs, which shows the strong dependence of the TDX on the α -clustering structure in ^{10}Be . Another important finding is the peripheral property of the knockout reaction, which guarantees high selectivity for probing the α -cluster in the surface region and allows one to use $y^{\text{app}}(a)$. Using our framework, we may directly relate the microscopic description of α -clustering structure to the reaction observables in the $(p, p\alpha)$ knockout reaction,

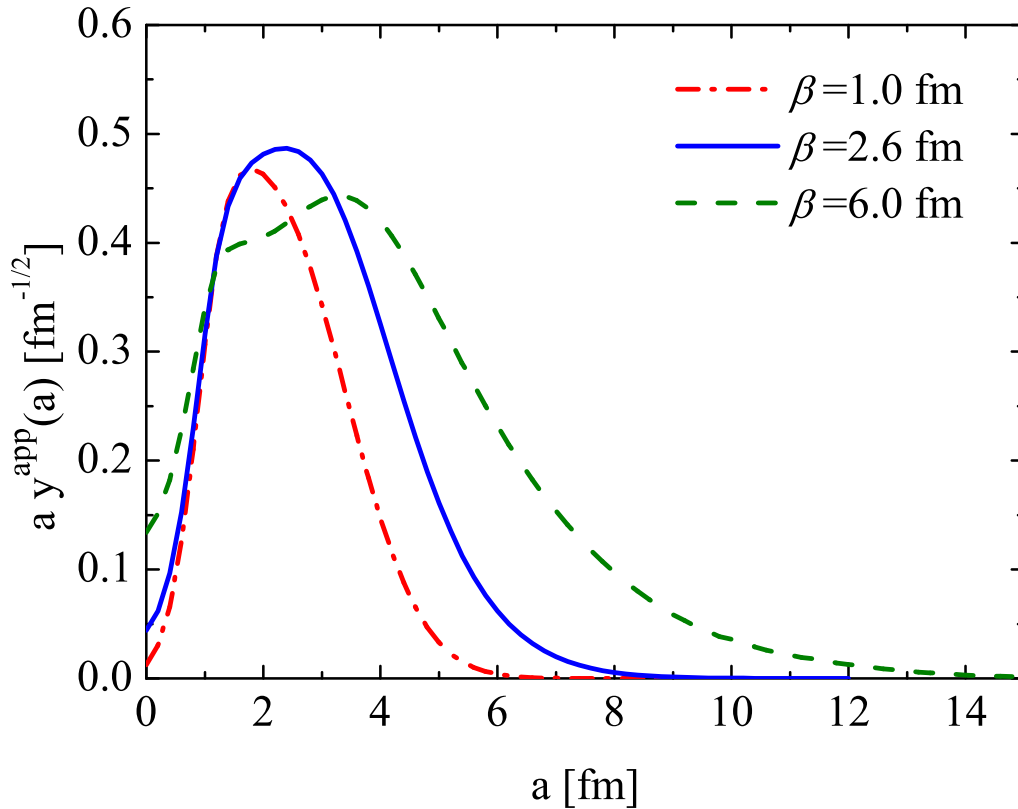


FIG. 3: The approximated RWA of ^{10}Be nucleus for the three values of $\beta_{\alpha,z}$. (Color online)

and provide sensitive manifestation of α -clustering in the ^{10}Be nucleus. In future, it is appealing and hopeful to extend this microscopic framework for systematic studies of α -clustering states.

Acknowledgments

The authors thank K. Minomo, Y. Chazono, and N. Itagaki for valuable discussions. The computation was carried out with the computer facilities at the Research Center for Nuclear Physics, Osaka University. This work was supported in part by Grants-in-Aid of the Japan Society for the Promotion of Science (Grants No. JP16K05352 and No. JP15J01392).

-
- [1] H. Horiuchi, K. Ikeda, and K. Katō, *Progress of Theoretical Physics Supplement* **192**, 1 (2012).
 - [2] M. Freer, H. Horiuchi, Y. Kanada-En'yo, D. Lee, and U.-G. Meißner, arXiv:1705.06192 (2017).
 - [3] S. Okabe, Y. Abe, and H. Tanaka, *Prog. Theor. Phys.* **57**, 866 (1977).
 - [4] M. Seya, M. Kohno, and S. Nagata, *Prog. Theor. Phys.* **65**, 204 (1981).
 - [5] P. Descouvemont, *Phys. Rev. C* **39**, 1557 (1989).
 - [6] W. von Oertzen, *Z. Phys. A* **354**, 37 (1996).
 - [7] K. Arai, Y. Ogawa, Y. Suzuki, and K. Varga, *Phys. Rev. C* **54**, 132 (1996).
 - [8] A. Doté, H. Horiuchi, and Y. Kanada-En'yo, *Phys. Rev. C* **56**, 1844 (1997).
 - [9] Y. Kanada-En'yo, H. Horiuchi, and A. Doté, *Phys. Rev. C* **60**, 064304 (1999).
 - [10] Y. Ogawa, K. Arai, Y. Suzuki, and K. Varga, *Nucl. Phys. A* **673**, 122 (2000).
 - [11] N. Itagaki and S. Okabe, *Phys. Rev. C* **61**, 044306 (2000).
 - [12] P. Descouvemont, *Nucl. Phys. A* **699**, 463 (2002).
 - [13] M. Ito, K. Katō, and K. Ikeda, *Phys. Lett. B* **588**, 43 (2004).

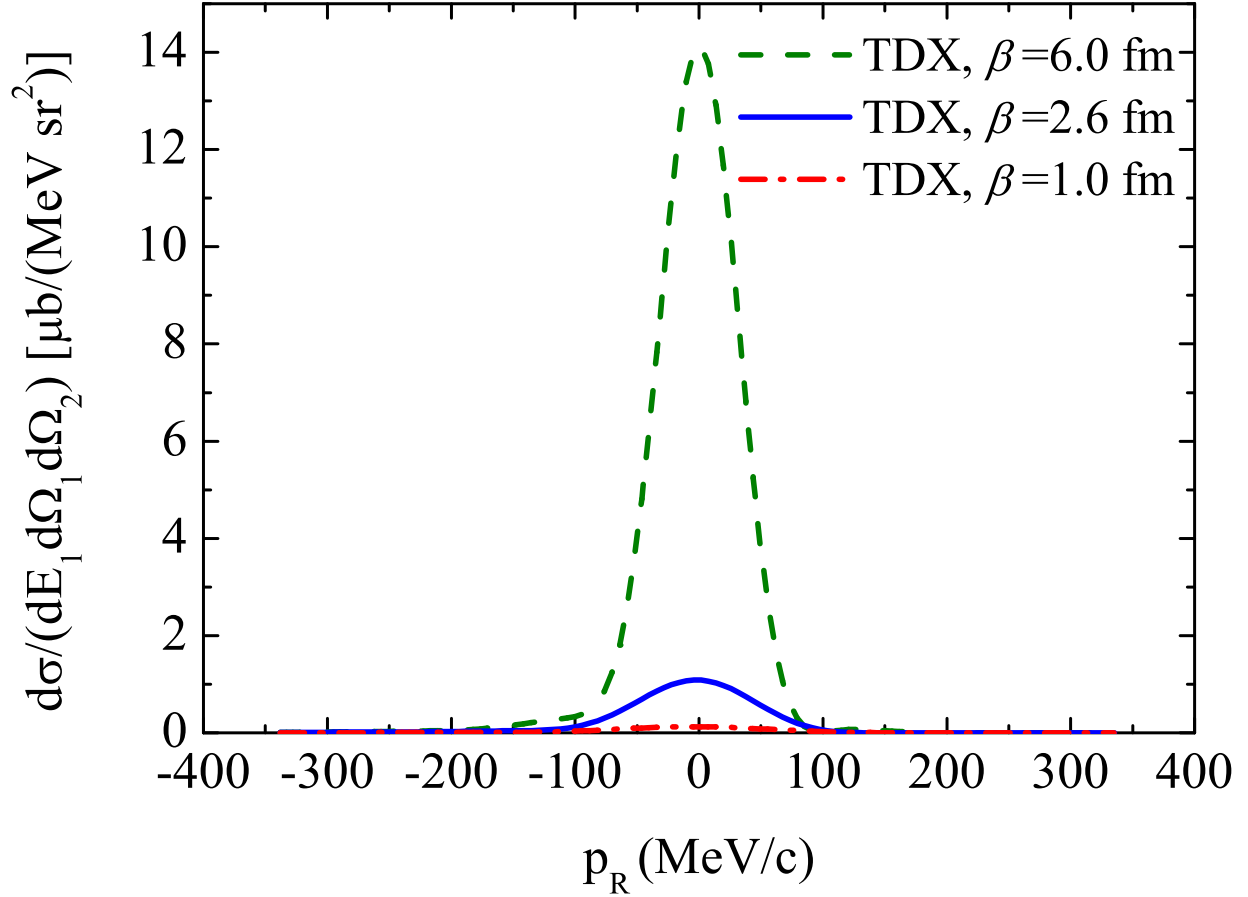


FIG. 4: The TDX of the $^{10}\text{Be}(p,p\alpha)^6\text{He}$ reaction at 250 MeV. Kinetic energy of particle 1 is fixed at 180 MeV and its emission angle is set to $(\theta_1, \phi_1) = (60.9^\circ, 0^\circ)$. ϕ_2 for particle 2 is fixed at 180° and θ_2 is varied around 51° . P_R is the recoiled momentum. (Color online)

- [14] W. von Oertzen, M. Freer, and Y. Kanada-En'yo, *Phys. Rep.* **432**, 43 (2006).
- [15] F. Kobayashi and Y. Kanada-En'yo, *Phys. Rev. C* **86**, 064303 (2012).
- [16] M. Ito, and K. Ikeda, *Rep. Prog. Phys.* **77**, 096301 (2014).
- [17] M. Lyu, Z. Ren, B. Zhou, Y. Funaki, H. Horiuchi, G. Röpke, P. Schuck, A. Tohsaki, C. Xu, and T. Yamada, *Phys. Rev. C* **91**, 014313 (2015).
- [18] M. Lyu, Z. Ren, B. Zhou, Y. Funaki, H. Horiuchi, G. Röpke, P. Schuck, A. Tohsaki, C. Xu, and T. Yamada, *Phys. Rev. C* **93**, 054308 (2016).
- [19] A. Tohsaki, H. Horiuchi, P. Schuck, and G. Röpke, *Phys. Rev. Lett.* **87**, 192501 (2001).
- [20] Y. Funaki, H. Horiuchi, and A. Tohsaki, *Prog. Part. Nucl. Phys.* **82**, 78 (2015).
- [21] Y. Funaki, *Phys. Rev. C* **92**, 021302 (2015).
- [22] Y. Funaki, *Phys. Rev. C* **94**, 024344 (2016).
- [23] B. Zhou, A. Tohsaki, H. Horiuchi, and Z. Ren, *Phys. Rev. C* **94**, 044319 (2016).
- [24] T. Fukui, Y. Taniguchi, T. Suhara, Y. Kanada-En'yo, and K. Ogata, *Phys. Rev. C* **93**, 034606 (2016).
- [25] K. Yoshida, K. Minomo, and K. Ogata, *Phys. Rev. C* **94**, 044604 (2016).
- [26] K. Yoshida, K. Ogata, and Y. Kanada-En'yo, arXiv:1712.09079 (2017).
- [27] P. G. Roos, N. S. Chant, A. A. Cowley, D. A. Goldberg, H. D. Holmgren, and R. Woody, III, *Phys. Rev. C* **15**, 69 (1977).
- [28] A. Nadasen, N. S. Chant, P. G. Roos, T. A. Carey, R. Cowen, C. Samanta, and J. Wesick *Phys. Rev. C* **22**, 1394 (1980).
- [29] T. A. Carey, P. G. Roos, N. S. Chant, A. Nadasen, and H. L. Chen, *Phys. Rev. C* **29**, 1273 (1984).
- [30] C. W. Wang, P. G. Roos, N. S. Chant, G. Ciangaru, F. Khazaie, D. J. Mack, A. Nadasen, S. J. Mills, R. E. Warner, E. Norbeck, F. D. Becchetti, J. W. Janecke, and P. M. Lister, *Phys. Rev. C* **31**, 1662 (1985).
- [31] A. Nadasen, P. G. Roos, N. S. Chant, C. C. Chang, G. Ciangaru, H. F. Breuer, J. Wesick, and E. Norbeck, *Phys. Rev. C* **40**, 1130 (1989).
- [32] J. Mabiala, A. A. Cowley, S. V. Försch, E. Z. Buthelezi, R. Neveling, F. D. Smit, G. F. Steyn, and J. J. Van Zyl, *Phys. Rev. C* **79**, 054612 (2009).

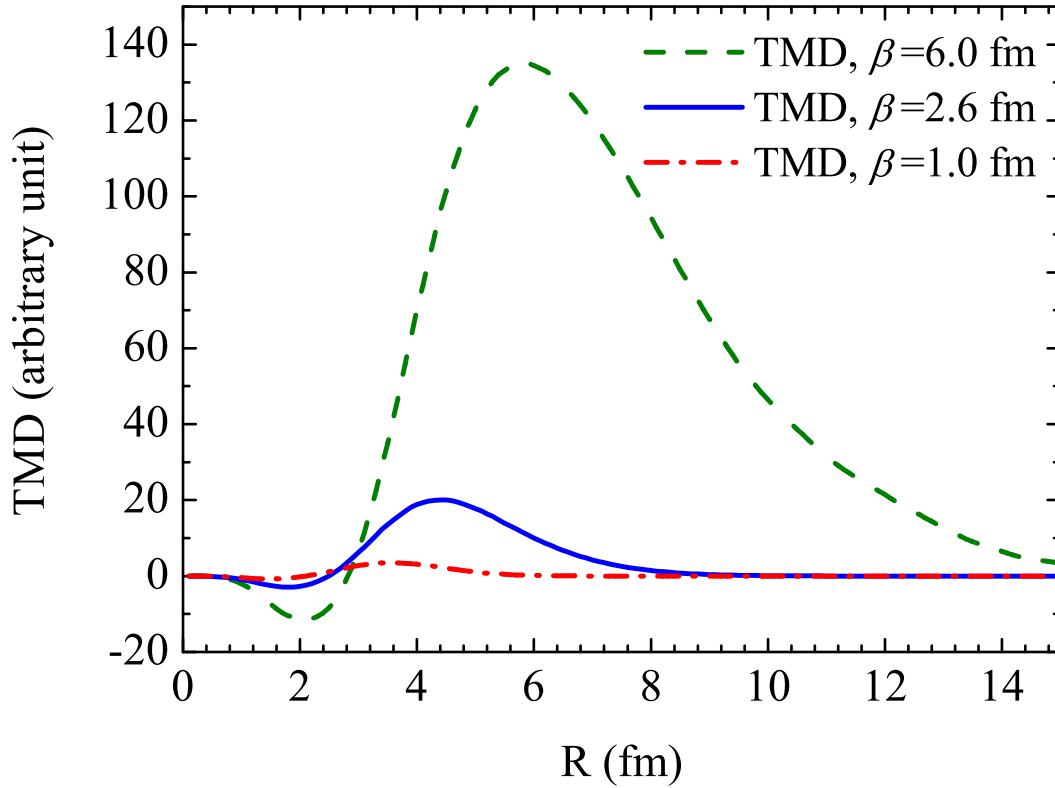


FIG. 5: TMD of the $^{10}\text{Be}(p,p\alpha)^6\text{He}$ reaction at 250 MeV for $P_R = 0$. (Color online)

(2009).

- [33] T. Wakasa, K. Ogata, and T. Noro, *Progress in Particle and Nuclear Physics* **96**, 32 (2017).
- [34] Y. Kanada-En'yo and H. Horiuchi, *Prog. Theor. Phys. Suppl.* **142**, 205 (2001).
- [35] Y. Kanada-En'yo, M. Kimura, and A. Ono, *Prog. Theor. Exp. Phys.* **2012**, 01A202 (2012).
- [36] H. Horiuchi, K. Ikeda, and K. Katō, *Prog. Theor. Phys. Suppl.* **192**, 1 (2012).
- [37] Z. Yang (private communication).
- [38] Q. Zhao, Z. Ren, M. Lyu et al., *to be submitted* (2017).
- [39] P. Ring and P. Schuck, *The Nuclear Many-Body Problem* (Springer-Verlag, New York, 1980).
- [40] Y. Kanada-En'yo, T. Suhara, and Y. Taniguchi, *Prog Theor Exp Phys* **2014**, 073D02 (2014).
- [41] D. M. Brink, *International School of Physics "Enrico Fermi", XXXVII*(Academic Press, New York 1966), p. 247.
- [42] A. B. Volkov, *Nucl. Phys.* **74**, 33 (1965).
- [43] N. Yamaguchi, T. Kasahara, S. Nagata, and Y. Akaishi, *Prog. Theor. Phys.* **62**, 1018 (1979).
- [44] K. Amos, P. J. Dortmans, H. V. von Geramb, S. Karataglidis, and J. Raynal, in *Advances in Nuclear Physics*, edited by J. W. Negele and E. Vogt (Plenum, New York, 2000) Vol. 25, p. 275.
- [45] K. Egashira, K. Minomo, M. Toyokawa, T. Matsumoto, and M. Yahiro, *Phys. Rev. C* **89**, 064611 (2014).
- [46] W. Nörtershäuser, D. Tiedemann, M. Žáková *et al.*, *Phys. Rev. Lett.* **102**, 062503 (2009).